

Steered Molecular Dynamics Simulations Predict Conformational Stability of Glutamate Receptors

Maria Musgaard and Philip C. Biggin**

Department of Biochemistry, University of Oxford, Oxford, United Kingdom

ABSTRACT

The stability of protein-protein interfaces can be essential for protein function. For ionotropic glutamate receptors, a family of ligand-gated ion channels vital for normal function of the central nervous system, such an interface exists between the extracellular ligand binding domains (LBDs). In the full-length protein, the LBDs are arranged as a dimer of dimers. Agonist binding to the LBDs opens the ion channel, and briefly after activation the receptor desensitizes. Several residues at the LBD dimer interface are known to modulate desensitization, and conformational changes around these residues are believed to be involved in the state transition. The general hypothesis is that the interface is disrupted upon desensitization, and structural evidence suggests that the disruption might be substantial. However, when crosslinking the central part of this interface, functional data suggest that the receptor can still undergo desensitization, contradicting the hypothesis of major interface disruption. Here, we illustrate how opening the dimer interface using steered molecular dynamics (SMD) simulations, and analyzing the work values required,

provides a quantitative measure for interface stability. For one subtype of glutamate receptors, which is regulated by ion binding to the dimer interface, we show that opening the interface without ions bound requires less work than with ions present, suggesting that ion binding indeed stabilizes the interface. Likewise, for interface mutants with longer-lived active states, the interface is more stable, while the work required to open the interface is reduced for less active mutants. Moreover, a crosslinked mutant can still undergo initial interface opening motions similar to the native receptor and at similar energetic cost. Thus, our results support that interface opening is involved in desensitization. Furthermore, they provide reconciliation of apparently opposing data and demonstrate that SMD simulations can give relevant biological insight into longer timescale processes without the need for expensive calculations.

INTRODUCTION

Excitatory signaling in the central nervous system (CNS) is heavily dependent on ionotropic glutamate receptors (iGluRs), a family of ligand-gated cation channels activated by the excitatory neurotransmitter glutamate. The iGluRs are furthermore crucial for e.g. learning and memory formation. Because of their widespread presence and effects, iGluRs are also potential targets in a wide variety of diseases and conditions affecting the CNS, e.g. epilepsy, stroke and Alzheimer's disease¹. Three main families of iGluRs are generally considered, namely kainate (KA), α -amino-3-hydroxy-5-methyl-4-isoxazolepropionic acid (AMPA) and N-methyl-D-aspartate (NMDA) receptors. AMPARs and KARs are more similar to each other than to NMDARs and are often described as non-NMDARs. AMPARs and KARs have sequence

identities of around 40%, whereas NMDARs show less than 30% sequence identity to the non-NMDARs².

The first close to full-length iGluR structure to be determined was an AMPAR GluA2 construct from Sobolevsky *et al.* in 2009 (Figure 1A)³. The structure is composed of four chains forming a tetrameric complex with a transmembrane domain (TMD) and two extracellular domains, an amino-terminal domain (ATD) and a ligand-binding domain (LBD). The TMD shows four-fold symmetry whereas the ATD and the LBD are both composed of a dimer of dimers. The LBD is further divided into the two lobes of each monomer, the upper lobe (D1) and the lower lobe (D2), together making up the LBD clamshell. Binding of an agonist to the LBD activates the channel by promoting closure of the clamshell which in turn is believed to exert a pull on the linker connecting the LBD to the channel-lining helix and thereby open the channel, allowing for influx of sodium ions (and, depending on the specific nature of the channel, calcium ions). Briefly after channel activation, at least for non-NMDARs, the receptor enters a desensitized state in which the agonist remains bound but the channel closes off. The receptor cannot be re-activated whilst residing in the desensitized state, but rather it has to return to the resting state. Thus, the functional cycle can overall be described by three states; resting, active and desensitized. Understanding the structural transitions, and perhaps especially the transition from active to desensitized, is important from a pharmacological perspective. Small-molecule allosteric modulators of this transition, either positive, stabilizing the active state and thus prolonging the signal, or negative, promoting desensitization and thereby reducing the signal, could be valuable drugs helping to fine-tune signaling rather than overactivating or constitutively blocking with full agonists or full antagonists¹.

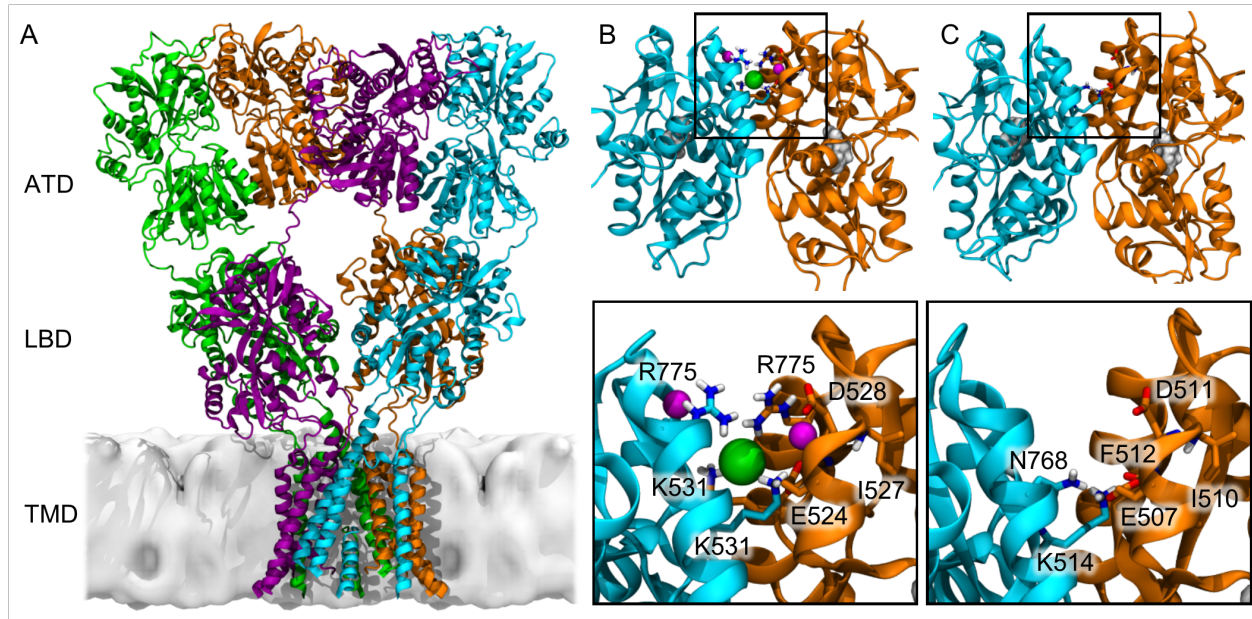


Figure 1. Overall structure of ionotropic glutamate receptors and structure of the ligand binding domain dimer interface. (A) The first full-length structure of an iGluR, GluA2, in complex with a competitive antagonist (not shown) and thus believed to be in a resting state with the ion channel closed (PDB ID 3KG2³). The approximate membrane position is predicted by the Orientations of Proteins in Membranes database⁴. (B) A KAR GluK2 LBD dimer (top) in the active state with glutamate bound (white surface representation) (PDB ID 3G3F⁵). The two-lobed structure is often described as a clamshell with D1 referring to the upper lobe and D2 to the lower, and thus the dimer interface is also referred to as the D1D1 interface. An enlarged view of the apex of the interface (bottom) shows the sodium (purple) and chloride (green) ion binding sites. Residues surrounding the ions are shown in licorice. For clarity, only residues around one of the two symmetric sodium ion binding sites are shown. (C) Same representations as (B) but for an AMPAR GluA2 LBD dimer (PDB ID 2UXA⁶). GluA2 does not require ion binding at the dimer interface, instead a strong set of hydrogen bonds and ionic interactions is formed across the interface. The numbering system applied for both GluK2 and GluA2 throughout the paper

corresponds to the full length peptide, including the 21 amino acids residues of the signal peptide. To convert to residue numbers used for the mature peptide, subtract 21 from the numbers given here.

The LBD dimer interface (Figure 1B and 1C) has long been known to be involved in the transition between the active and desensitized states as stabilization of this interface, by either mutations or allosteric modulators, reduces the rate of desensitization⁷. Correspondingly, destabilization of the interface enhances desensitization^{5,7}; for example in GluA2 where various interface mutants are known to increase the rate of desensitization, e.g. K514A, E507A, and N768A⁸. The first structural insight into the desensitization mechanism came in 2006 from Armstrong *et al.*⁹ based on crystallizing a mutant LBD dimer. They realized that two crosslinked GluA2 mutants, G746C and S750C, were trapped in an inactive state unless dithiothreitol (DTT) was co-applied with glutamate to break the disulfide bonds. Thus, it seemed likely that this inactive state would correspond to the desensitized state, and they crystallized the LBD dimer of this mutant. The crystal structure revealed that the apex of the upper D1D1 interface has opened, underlining that the D1D1 interface was important for desensitization. Several years later, Schauder *et al.*¹⁰ obtained density maps at 21 Å resolution for full-length KAR GluK2 receptors in the resting and the desensitized states using cryoelectron tomography. These maps suggest that the D1D1 interface ruptures even more than indicated from the crosslinked structures as the LBD dimers fully disassemble to obtain four-fold symmetry at the LBD level in the desensitized state. Higher-resolution structures were published in 2014 from two different laboratories, again suggesting that the D1D1 interface opens more completely than seen in the crosslinked structure^{11,12}. One structure, from Dürr *et al.*¹¹ determined to a resolution of around 8 Å, shows an

LBD arrangement where one of the dimers is completely disassembled, whereas the other dimer is found in a conformation resembling the disulfide-linked structures from 2006⁹. The structure was bound to a partial agonist and believed to be in a desensitized state. The other presumably desensitized structure, determined by Meyerson *et al.*¹² to a resolution of 7.6 Å, showed both of the LBD dimers having completely disassembled, and the LBD level of the receptor is observed to have four-fold symmetry as opposed to the two fold symmetry generally seen for the extracellular domains in the resting state. Meyerson *et al.* suggest that the crosslinked structures from 2006 may likely be intermediates towards the fully desensitized state but where the LBDs cannot move any further because of the crosslink. Furthermore, both Meyerson *et al.* and Dürr *et al.* suggest that the “desensitized state” may cover several different conformations, which is supported by their cryo-electron microscopy data. A potential restriction for the full-length structures is that no auxiliary proteins are present, and these could potentially bind to and limit the motion of the LBDs. Another structure published in 2014 was also suggested to be a desensitized state¹³. This structure is, however, very different from the Meyerson and Dürr structures in that the LBD dimers have not dissociated and the arrangement appears to be more similar to the resting state. The authors note that the state may also be a “pre-open” state but since such a state is expected to be short-lived and quite unstable, they suggest that capturing this state in a crystal is relatively unlikely, unless perhaps the crystallographic contacts provide significant extra stabilization to this state¹³. To investigate the dynamics of the functional cycle, Yelshanskaya *et al.* further introduce cysteine crosslinks at various sites in the LBD dimer along the interface¹³. Surprisingly, they find that K514C forms crosslinks, and that these crosslinks do not seem to affect the ability of the receptor to enter either the active or the desensitized state. Rather, it behaves similar to the GluA2 WT. This is particularly surprising since Armstrong *et*

*al.*⁹ found that using MTS reagents to crosslink the interface at the level of K514 would lead to potentiation of the current provided that the MTS reagent was reasonably short. Instead of interface opening, Yelshanskaya *et al.* suggest that a rotation of the two LBDs in the dimer relative to each other is involved in the desensitization process¹³.

Overall, the amount of structural information for the iGluRs has increased tremendously over the last few years. However, the large-scale conformational changes that occur during the functional cycle are still not well understood. What is clear is that a considerable amount of control in these processes is held within the LBD dimer interface. One way of gaining insight into the conformational changes undergone in the transition from the active to the desensitized state is by computational modelling. However, modelling the full-length receptor in the active state suffers from the fact that the structure of the active state has not yet been solved to atomistic resolution. Yet, earlier studies have illustrated that much can be learned from studying the isolated LBD, either in the monomeric^{14–16} or the dimeric form^{17–20}. Thus, we wanted to explore with computational modelling exactly how that control is manifested. In particular, we wanted to investigate whether a fuller understanding of the interactions across the interface could be quantified to the extent that predictions could be made about whether a mutation would enhance or reduce the rate of desensitization. Additionally, we wanted to examine whether we could rationalize the data for the GluA2 K514C crosslinked receptor, which appear to desensitize in a manner similar to WT GluA2.

Kainate receptors are different from the two other iGluR families in that they require binding of extracellular ions to the LBD dimer interface to activate²¹. We have previously proposed that the binding of these ions to GluK2 stabilizes the interface and that ion release destabilizes the interface, favoring desensitization¹⁹. Thus, we first examined longer time scale MD simulations

of a GluK2 LBD dimer in the “active” conformation, analyzing the effect of spontaneous ion release during unbiased simulations. This allowed us to identify a collective variable to be used for Steered MD (SMD), in which we, by adding external forces, could drive the active LBD dimer conformation towards a potentially “desensitized” conformation. Obtaining the fully disassembled LBD dimers observed by Meyerson *et al.*¹² and Dürr *et al.*¹¹ would require a very complex biasing scheme. Here we focused on describing the initial step in the desensitization process in an efficient manner, targeting a plausible initial part of the conformational change. SMD simulations allow one to quantify the work required to move along a collective variable and thus provide a way to examine how residue composition influences the work profile. We applied this method to GluK2 kainate receptors, GluA2 AMPA receptors and mutants of both, and finally to the crosslinked K514C GluA2 receptor. We found that the work values obtained from SMD simulations allowed us to distinguish between stabilizing and destabilizing mutants. Moreover, in SMD simulations the crosslinked K514C GluA2 receptor was still capable of undergoing interface opening in a similar way to the WT and thus the crosslinked results do not contradict the general hypothesis of interface opening being involved in desensitization.

METHODS

Protein structures

For the GluK2 simulations, we used four different crystal structure models; a WT model (PDB ID 3G3F, 1.38 Å⁵), a Y521C/L783C mutant (PDB ID 2I0C, 2.25 Å²²), and a D776K mutant²³ with (PDB ID 2XXW, 2.3 Å) or without (PDB ID 2XXX, 2.1 Å) a chloride ion bound. All structures were LBD dimers with glutamate bound to each of the chains. The dimers showed a

similar overall conformation though the orientation of the two chains in the disulfide-linked double mutant was slightly different from the others. The terminals were trimmed such that residue 432 was the first included and residue 799 the last for each structure. Two isopropyl alcohol molecules were deleted from the WT structure, while ions (sodium and chloride for 3G3F and chloride for 2XXW), crystallographically resolved water molecules and bound glutamate were used together with the protein chains for constructing the simulation systems. For the L783C mutant, the structure was based on the 3G3F structure to which the leucine to cysteine mutation was added manually by editing the pdb file. For WT simulations without bound ions, the crystallographically resolved sodium and chloride ions were deleted before system setup.

For the GluA2 simulations, chains A and C from the flip R764 LBD structure was used (PDB ID 2UXA, 2.38 Å⁶). The unedited R764 was edited manually to G764 and the bound zinc ions were deleted. The LBD dimer, bound glutamate ligands and crystallographically resolved water molecules were used to construct systems for simulations. The L772A mutant structure was based on 2UXA with the leucine to alanine mutation added manually. For the K514C mutant in the reduced state, the lysine residues were mutated to cysteine using the Mutagenesis Wizard in PyMOL (The PyMOL Molecular Graphics System, Version 1.4 Schrödinger, LLC). However, this insertion of cysteine residues did not allow the side chain Sγ atoms to get close enough for formation of a disulfide crosslink. Thus, the K514C model in the reduced state was refined using MODELLER v 9.12²⁴ by keeping the whole model restrained except for the inserted cysteine residues and the four neighboring residues to allow for formation of the disulfide crosslink.

The LBD dimers with ligands, crystallographically resolved water molecules and, if required, ions were inserted into a cubic (100 Å)³ water box and the systems were neutralized and 150 mM NaCl was added. The OPLS force field^{25,26} was used along with the TIP3P water model²⁷.

MD simulations

MD simulations were performed in Gromacs 4.6²⁸. First, the systems were energy minimized until no forces on any atom exceeded 100 kJ/mol/nm. Following this, two short restrained simulations were performed with position restraints on the protein heavy-atoms using a force constant of 1000 kJ/mol/nm². First, 200 ps of MD simulation was run in the NVT ensemble, maintaining the temperature at 300 K using a Berendsen thermostat²⁹. The systems were simulated with periodic boundary conditions, and the cutoff for van der Waals interactions and short-range electrostatic interactions were 10 Å. The particle mesh Ewald (PME) method^{30,31} was employed to account for long-range electrostatics. The LINCS algorithm³² was used to treat all bonds as constraints, allowing a time step of 2 fs. Subsequently, another 200 ps of restrained MD simulation was performed, now in the NPT ensemble, keeping the pressure at 1 bar by applying a Berendsen barostat²⁹. Finally, all restraints on the protein were removed and production run was performed in the NPT ensemble using the settings described above. Each setup was repeated two to four times for 100-500 ns.

SMD simulations

SMD simulations were performed using the PLUMED 1.3 plugin³³ for Gromacs 4.6²⁸. The collective variable (CV) was the distance across the apex of the interface. The apex of the interface was for each GluK2 chain defined as the center of mass of the C_α atoms of residues K525, V526, I527, M770, G771, S772, P773, Y774, R775 and D776. Thus, the CV was the distance across the dimer interface between the center of mass of C_α atoms of these residues. For GluA2 the equivalent residues were used: E508, V509, I510, K759, G760, S761, S762, L763,

G764 and T765. The CV was steered towards a distance of 25 Å using a force constant of 1000 kJ/mol/nm² and a constant velocity of 1 Å/ns. To avoid problems caused by the periodic boundary conditions when some of the atoms in the CV leave the simulation box, the ALIGN_ATOMS keyword was used to keep the atoms of the CV together. Two SMD simulations were performed for each unbiased repeat from snapshots at either 0 ns, 50 ns or 100 ns. Work values were used as reported in the output COLVAR files produced by PLUMED.

Analysis

The output trajectories were analyzed using VMD³⁴ and analysis tools of Gromacs²⁸. Statistical comparisons of work averages were performed using two-tailed two-sample *t* tests assuming unequal variance of the data sets. $P < 0.05$ was considered statistically significant.

RESULTS

Ion release in unbiased simulations of GluK2 promoted interface opening

GluK2 kainate receptors are dependent on binding of extracellular ions for activation²¹. A chloride ion binding site and two symmetrical sodium ion binding sites have been identified at the apex of the LBD dimer D1D1 interface (Figure 1B)^{17,35}. We have previously suggested that GluK2 may desensitize only upon release of interface bound cations and, furthermore, that desensitization is promoted when glutamate binds to an ion-free state¹⁹. As ion binding or unbinding is a property easy to assess, we expected that the GluK2 LBD dimer would be a good model system to investigate initial conformational changes involved in desensitization.

To explore the stability of the GluK2 LBD dimer interface in longer time-scale MD simulations, we performed four 500 ns repeats of a WT system. For one of these simulations, the ions at the interface remained bound or were exchanged throughout the simulation and the protein remained conformationally stable (WT_a, see root mean square deviation (RMSD) and ion distances in Figure S1 and S2, respectively). For another simulation (WT_b), the LBD clamshell of one chain of the dimer opened up completely and exposed the bound glutamate ligand to the solvent while the LBD of the other chain also opened but to a smaller extent (data not shown). This explains the large RMSD for the second simulation. For the remaining two simulations (WT_c and WT_d), both lost the bound ions during the 500 ns of simulation, however, the RMSD values did not suggest any major conformational changes. In general, these trajectories corresponded well to our previous unbiased simulations of iGluR WT LBD dimers with the dimers being relatively stable and glutamate remaining in the binding pocket^{19,20}, with the exception that WT_b showed clamshell opening.

To identify potential collective motions that could suggest initial motions involved in desensitization, we performed principal component analysis of the four 500 ns trajectories. We studied the most important principal components (PCs), especially focusing on potential differences between the simulation in which the ions remained bound (WT_a) and the two simulations where the ions were released during the simulation (WT_c and WT_d), as we have previously suggested that the ion release would lead to desensitization¹⁹. Within the ten PCs which contributed the most to the observed dynamics, a number of modes for the trajectories in which ions were released, including PCs 2 and 3, contained a component of D1D1 interface opening (Figure 2A and Movie S1). This motion was less pronounced for the trajectory in which the ions remained bound. The first PC for both of these two simulations, WT_c and WT_d, was

dominated by more local loop motions. For the trajectory in which the LBD clamshells opened, the clamshell opening motions heavily dominated the PCs. As this process illustrated deactivation rather than desensitization, we did not analyze this result further. To evaluate the importance of D1D1 interface opening further, we measured the distance across the apex of the interface (defined as the distance between the center of mass of the C α atoms of residues 525-527 and 770-776 in each chain) and investigated whether this distance was dependent on the number of sodium ions bound. As evident from Figure 2B, the interface opened up and packed less tightly after sodium ions unbound. Thus, unbiased simulations of the GluK2 WT suggested that random ion unbinding promoted opening motions at the apex of the D1D1 interface. Furthermore, longer time-scale unbiased simulations of the GluK2 WT LBD dimer indicate that interface opening motions become more pronounced upon unbinding of interface cations, an unbinding we have previously suggested to be a necessity for desensitization¹⁹. To explore this motion further, we performed SMD simulations, in which external forces are added to atom or groups of atoms to induce a given event. In this case, SMD simulations were used to drive the LBD dimer to a state with a more open interface than what was obtainable by unbiased MD simulations at the ns time scale.

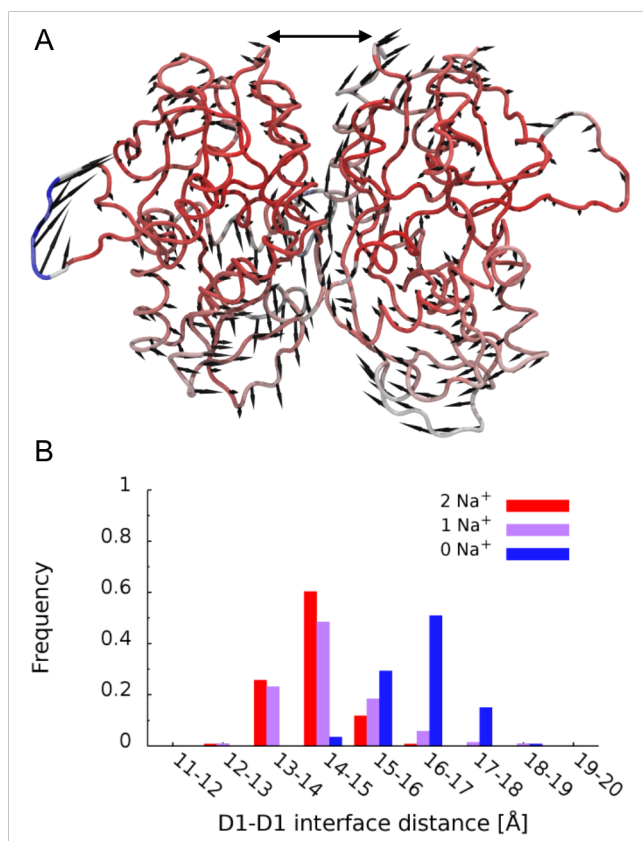


Figure 2. Interface opening, identified through principal component analysis, is coupled to ion occupancy. (A) The second PC for a simulation in which the ions have been released. A component of dimer interface opening is observed, indicated by a double-headed arrow. A number of PCs among the first ten include a similar component of interface opening motion. The backbone is colored by fluctuation, with red being least flexible and blue being most flexible. (B) Degree of interface opening relative to the number of sodium ions bound. The data was collected for 4 x 500 ns (in total 40,000 frames) of unbiased simulations for GluK2 WT in which all four simulations had ions bound initially.

SMD opened the D1D1 interface to a degree comparable to crosslinked “desensitized”

GluA2 structure

To test whether SMD could be a useful methodology to study the interface opening of the GluK2 LBD dimer, we took a snapshot after 50 ns of unbiased MD simulation for the trajectory from above in which the ions remained bound (WT_a) and performed an SMD simulation. In the simulation, the interface was pushed open at the top, using a collective variable (CV) describing the interface distance at the D1D1 interface apex (Figure 3A). The final snapshot from the SMD simulation was compared to the GluK2 crystal structure (Figure 3B) and it was clear that the apex of the interface was greatly opened. The overall conformation from the SMD output was perhaps slightly different from what one would expect at first. Instead of the two chains merely being pushed apart along the CV, the dimer interface had opened at the apex but the bottom remained closely packed even though no restraints were applied to this part of the dimer. Furthermore, the obtained conformation was, reassuringly, similar to the crosslinked “desensitized” GluA2 structure⁹, despite not using any information from this structure in the simulation setup (Figure 3C). This suggested that the defined CV, and thus the point of force application, did not give rise to unphysical conformational changes. The increased resemblance of the “desensitized” GluA2 structure and at the same time the increased deviation from the active GluK2 structure during interface opening was also clear from calculating the RMSD relative to each of these two crystal structures (Figure 3D). As the interface opened during the SMD simulation, the structure moved further away from the active state (increasing RMSD along the x-axis) and closer to the “desensitized” state (decreasing RMSD along the y-axis). The fact that the SMD simulation produced an output structure which was similar to a previously and independently obtained crystal structure suggested that SMD simulations provided a way of

obtaining further insight into the initial D1D1 interface opening which is likely involved in desensitization and thus highly relevant for the overall receptor mechanism.

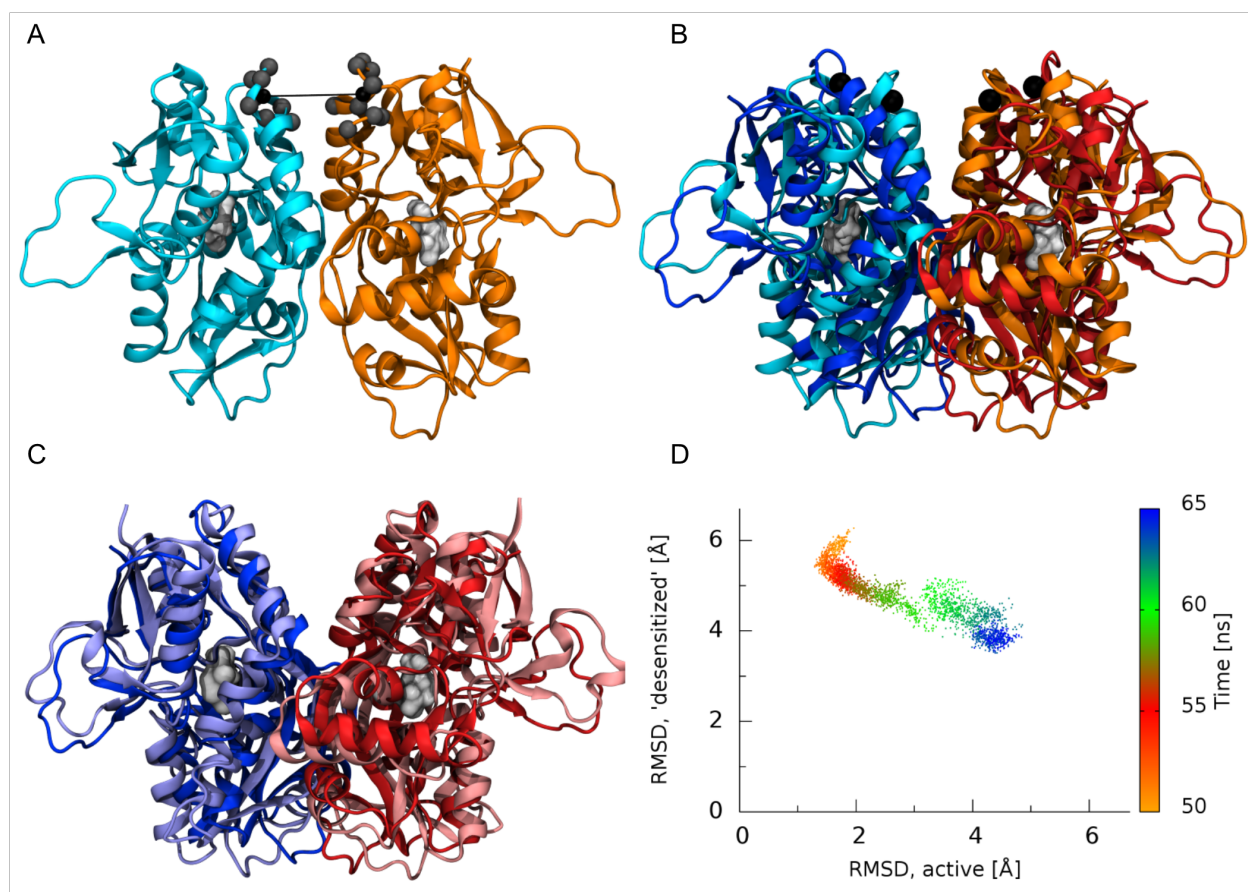


Figure 3. Steered MD simulations induce desensitization motions for the active GluK2 LBD dimer. (A) The GluK2 LBD dimer with the collective variable used for SMD simulations illustrated. The CV is defined as the distance between the centers of mass (black sphere) of the Cα atom of residues 525-527 and 770-776 in each chain (grey spheres). (B) Overlay of the SMD output structure (blue, red) with active crystal structure (cyan, orange, 3G3F⁵). (C) Overlay of the SMD output structure (blue, red) with the GluA2 AMPAR “desensitized” structure (pale blue, pale red, 2I3W⁹). (D) RMSD of the simulated structure relative to both the active GluK2 state (x-axis, the cyan/orange structure in panel (B)) and the “desensitized” GluA2 state (y-axis,

the pale blue/pale red in panel (C)). The simulation time is indicated by the color bar to the right (the SMD simulation starts after 50 ns of unbiased simulation). The RMSD is calculated for C-alpha atoms of residues which are equivalent between GluK2 and GluA2.

Ion dynamics varied between different repeats of SMD simulations

After confirming that SMD simulations may be valuable in studying conformational changes of the LBD dimer, we performed similar simulations starting from snapshots taken at 50 ns for the remaining three GluK2 WT LBD dimer simulations. The trajectories revealed that interface ions, perhaps not surprisingly, may unbind during the SMD simulations, and whether ions were bound or not seemed to affect the total work required to open the interface (see Figure 4). For some SMD simulations, all three interface ions were bound initially (simulation 1, 2 and 4, Figure 4) and for one of these, the ions remained bound relatively stably throughout the simulation (simulation 1). For simulation 2, one sodium ion unbound first (dark green curve, Figure 4), then the chloride ion (orange curve) and finally the other sodium ion (yellow curve). For simulation 4, the chloride ion unbound first (pink curve) and then a sodium ion (orange curve) shortly after. More work was required to open the interface for simulation 1 in which the ions remained bound more stably throughout the simulation relative to simulations 2 and 4. For the last shown example (simulation 3), one sodium ion had already been released before the start of the SMD simulation (i.e. within the first 50 ns of the unbiased MD simulation), and the other sodium ion seemed rather unstable (dark/light green curve, Figure 4). The work required to open the interface in simulation 3 was approximately halved relative to simulation 1 in which the ions remained bound. We thus wondered whether the state of ion binding at the initial snapshot of the

SMD simulation in general would affect the total amount of work required to open the interface, and thereby whether this could suggest that ion binding did indeed stabilize the D1D1 interface. However, we also wanted to test whether the differences in work could instead be explained by the differences in the starting value for the collective variable as this was under 14 Å in the simulation where the ions remained bound, and 15-16 Å in the other examples shown.

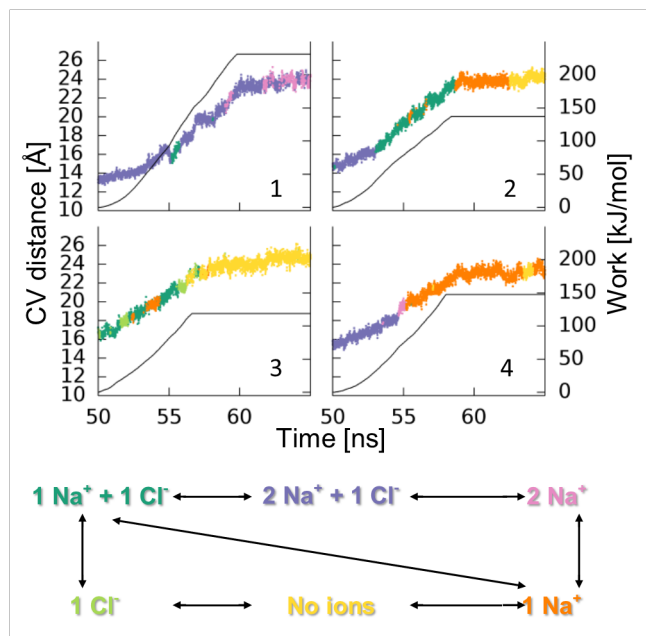


Figure 4. Ion dynamics vary between different SMD simulation repeats.

Four examples (simulation 1-4) of time-resolved ion-binding and unbinding events during SMD simulations. The collective variable (CV), i.e. the distance across the interface, is illustrated with colored curves where the colors illustrate which ions are bound to the interface following the color scheme below the graphs. The black lines illustrate the work required to open the interface.

More work was required to open the WT GluK2 LBD dimer interface if ions were bound initially

To investigate whether the ion binding state affected the work, we performed simulations in which the three interface-bound ions were removed before the start of the simulations, and used snapshots from here for SMD simulations as well. To determine whether the initial value of the CV influenced the work required to open the interface, we took, in addition to the snapshots at 50 ns, snapshots at 0 ns and 100 ns and used these for SMD simulation, both with and without ions bound. For each snapshot taken from unbiased simulations performed either with or without interface ions bound initially, we performed two repeats of the SMD simulations. Thus, we had eight repeats in total for each scenario at each of the chosen starting times. Average work values (\pm standard deviation) were calculated for each condition and a two-tailed t-test was used to determine whether potential differences between different starting conditions were statistically significant (Figure 5). The average work did not change significantly for snapshots taken at different time steps, neither for ion-bound nor for ion-unbound states. Thus, for the tested range of CV values, the average work did not change significantly with changes in initial CV values. For snapshots taken at 0 ns and at 50 ns, interface opening required significantly more work with ions present than without ions, however, for snapshots at 100 ns, the difference was no longer statistically significant. This is, however, explained by the fact that at this time, some ions have already unbound or at least been destabilized in their binding, so some of the states that are described as “ion-bound” could in principle more correctly be described as at least partly ion-free. This also explains the very large standard deviation on the average work for ion-bound states at snapshots taken at 100 ns (the work values range from 109-263 kJ/mol). Therefore, we concluded that taking snapshots at 50 ns for SMD simulations was the optimal to allow the protein structure to equilibrate but without risking too large deviation between the different snapshot. Despite the fact that some structural deviations are already present at 50 ns, the paths

followed in the SMD simulations are fairly similar (Figure S3). Additionally, we compared the PCs from the unbiased WT_c and WT_d simulations, which had components of interface opening, and despite the PC not capturing the full transition toward the more desensitized state, there is overlap between the motion captured by the PC analysis and the motion observed in the SMD simulations (Figure S3).

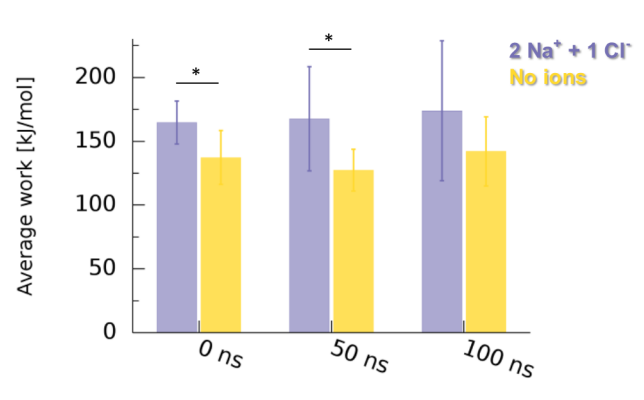


Figure 5. Binding of regulatory interface-bound ions stabilizes the LBD dimer interface. Average work values for opening the interface in GluK2 WT with (blue) or without (yellow) regulatory ions bound. The error bars show the standard deviation. Four unbiased repeats were simulated for each condition (with/without ions) and SMD was performed two times for each repeat, i.e. for each condition: $n = 8$ (4 snapshots \times 2 repeats). The average work did not change significantly for different starting times (minimum $p = 0.24$). The work required to open the interface is larger with ions bound than without at 0 ns ($p = 0.018$) and at 50 ns ($p = 0.038$) as indicated by * ($p < 0.05$). At 100 ns there is no significant difference between having ions or not ($p = 0.20$), probably because at this time, several ions have been destabilized in their binding.

These results suggested that, in addition to using SMD simulations to investigate the initial motions in desensitization, we could also use SMD simulations to investigate whether the LBD

dimer interface in a given condition was more or less stable relative to a reference by looking at the work required to open the interface. To examine whether the method could also be used to assess potential stabilization/destabilization caused by interface mutations, we looked at different GluK2 mutants.

Work values from SMD simulations can predict whether an interface mutation is stabilizing or destabilizing

We have previously studied different interface mutants for the GluK2 LBD dimer¹⁹ and we wanted here to investigate whether SMD simulations could predict whether a given mutation would be stabilizing or destabilizing relative to the WT receptor (Figure 6A). The D776K mutation (Figure 6B) has previously been shown to give a non-desensitizing phenotype, both in macroscopic³⁶ and single-channel¹⁹ experiments. The Y521C/L783C double mutant (Figure 6C) was first believed to be non-desensitizing as well²², but single-channel measurements have shown that it actually activates only poorly¹⁹. Finally, the L783C mutant (Figure 6D) has been illustrated to be non-functional despite good surface expression^{19,22}. For each of the mutants, we performed two repeats of unbiased MD simulation, took snapshots at 50 ns and performed two repeats of SMD simulation from each snapshot. The interface could open for all mutants, and we calculated the average work (\pm standard deviation) for each mutant (Figure 6E). The results showed that for the non-desensitizing mutant, D776K, more work was required to open the interface than for the WT, at least if D776K had the interfacial chloride ion bound (D776K+Cl). If the chloride ion was not bound (D776K-Cl), the work was comparable to the work required to open the WT interface in the presence of ions. For the Y521C/L783C double mutant and the L783C single mutant, both illustrating only little or no activity, the work required to open the

interface was less than for the WT, suggesting that the interface was destabilized. Thus, for the studied GluK2 mutants, the experimental evidence and the work values from SMD simulations agree on whether a given mutation is destabilizing the D1D1 interface and therefore whether the mutant will show poor activity. To investigate whether the same relationship could be identified for AMPARs, we tested the GluA2 WT along with a GluA2 mutant.

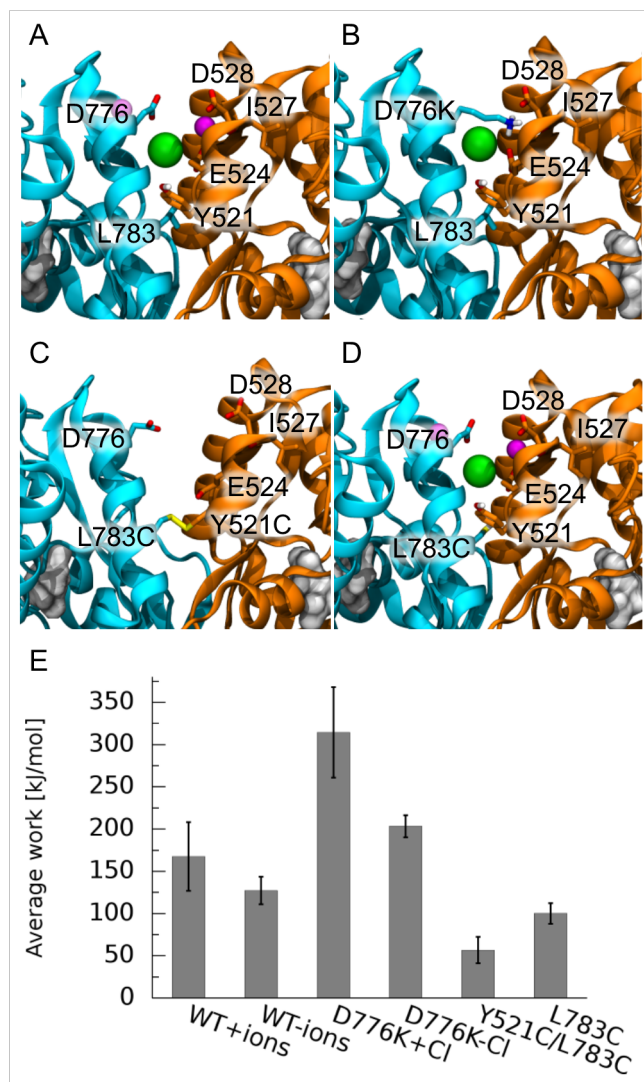


Figure 6. Work values from SMD simulations can predict the effect of interface mutations. (A)-(D) Interface structure for the GluK2 WT⁵ (A) and the three studied mutants D776K²³ (B), Y521C/L783C²² (C) and L783C (D). The mutations are symmetric but for clarity only shown in

one side. (E) Average work required to open the interfaces for GluK2 WT and mutants. All snapshots for SMD simulations are taken after 50 ns of unbiased simulation. For WT $n = 8$ and for mutants $n = 4$. The work required to open the interface is larger for WT with ions than for Y521C/L783C ($p = 0.0001$) and for L783C ($p = 0.003$). The work required to open the interface is larger for D776K with Cl^- than for WT with ions ($p = 0.0099$) but for D776K without Cl^- the average work is not significantly different from WT with ions ($p = 0.066$). This is not of concern as we believe that the WT is in principle non-desensitizing as long as ions remain bound.

SMD simulations can open GluA2 in a similar way to GluK2 and predict interface stability

Interface mutants affecting the receptor activity are also known for the AMPAR GluA2 receptors (e.g. ⁸). To test whether SMD simulations can be used for GluA2 in a way similar to GluK2 to assess the interface stability and thus the stability of the active state, we studied the WT GluA2 receptor along with the L772A mutant. The position of L772 is equivalent to L783 in GluK2 (Figure 6D). The L772A mutant does not respond to glutamate alone, however, it does activate after treatment with cyclothiazide, an allosteric modulator of AMPARs⁸. SMD simulations for the GluA2 WT opened the interface in a way similar to that observed for GluK2. The average work (\pm standard deviation) required to open the GluA2 WT interface was 100 ± 19 kJ/mol, whereas for the GluA2 L772A mutant it was 33 ± 7 kJ/mol (for WT $n = 8$ and for L772A $n = 4$). Thus, the work required to open the interface for the inactive L772A mutant was much reduced compared to the work required to open the dimer interface for the GluA2 WT ($p = 1 \cdot 10^{-5}$). This supports the notion that the L772A mutation heavily destabilizes the interface and explains why this mutant does not activate. Thus, for GluA2 AMPA receptors the SMD simulations can be used to assess interface stability in the same way as for GluK2 kainate

receptors. The interface destabilization was, however, also evident from unbiased simulations, illustrating interface opening for L772A (data not shown).

GluA2 receptors do not require the binding of extracellular ions to activate in order to stabilize the interface³⁷. Instead, GluA2 has an extra interaction across the dimer interface compared to GluK2, namely a hydrogen bond between N768 and E507 in addition to the conserved salt bridge between E507 and K514 (Figure 1C). For single mutants, taking out either of these residues speeds up desensitization⁸. The importance of this set of interactions was evident from our SMD trajectories (see Figure S4). In one of the WT simulations (referred to as WT_a), the E507-K514 interaction was only present in one side of the dimer for the snapshot at 50 ns used as initial structure for SMD simulation, while the E507-N768 interaction was missing for both chains. The work required to open the interface for the two repeats starting from this snapshot (average 71 kJ/mol) is significantly smaller ($p = 0.006$) than the work required to open the interface when all four of these interactions are present in the initial snapshots (109 kJ/mol, simulations WT_{b,d}, both repeats). Thus, for GluA2 we would suggest that for desensitization to happen, the interaction network across the interface should be broken, as it would be expected that the physiological pathway follows the path of least resistance.

To explore the importance of this set of interactions (E507-K514 and E507-N768) further, we simulated a triple mutant in which these three residues had all been exchanged for alanine (K514A/E507A/N768A). Surprisingly, no difference in terms of interface opening in unbiased simulations was found relative to the WT (data not shown). However, when we performed SMD simulations, we did indeed observe a difference relative to WT; the average work for opening the K514A/E507A/N768A interface was 45 ± 15 kJ/mol (significantly smaller than for WT ($p = 0.002$)). Thus, the interface is predicted to show a much reduced stability for the mutant which

agrees with electrophysiology which shows an almost 10-fold faster onset of desensitization for the mutant relative to the WT²⁰. For this mutant, the unbiased simulations at 100 ns timescale were not enough to reveal the instability of the interface, however, the destabilization was clearly evident from short SMD simulations.

Seeing that the interface opens in a similar way for GluA2 as for GluK2, and that the work required to open the interface can again be used to investigate effects of mutations, suggested to us that the interface opening is likely to be involved in the iGluR desensitization for non-NMDARs. However, based on different structural and functional evidence, it has also been suggested that the interface opening may in fact not be involved in desensitization, since GluA2 receptors crosslinked at the interface are still able to undergo desensitization¹³. Thus, to investigate what might happen to these receptors, we finally studied a crosslinked GluA2 mutant to see whether they would still be able to undergo interface opening.

Crosslinked GluA2 may still undergo initial interface opening

Though most structural evidence points towards LBD dimer interface opening being involved in desensitization, some functional data on crosslinked GluA2 receptors seem to contradict the hypothesis. Yelshanskaya *et al.*¹³ showed recently that a crosslinked GluA2 mutant, K514C (Figure 7A), maintains the ability to desensitize despite the conformational space of the LBD dimer interface presumably being very limited due to the crosslink. On the other hand, Armstrong *et al.*⁹ previously showed that crosslinking a GluA2 K514C mutant by the aid of small MTS reagents potentiates the equilibrium current. However, neither of the two papers show single-channel data for the mutants, which could potentially be helpful to explain the

apparent discrepancy. We investigated with SMD simulations whether the crosslinked K514C mutant could still undergo the presumed initial desensitization motions.

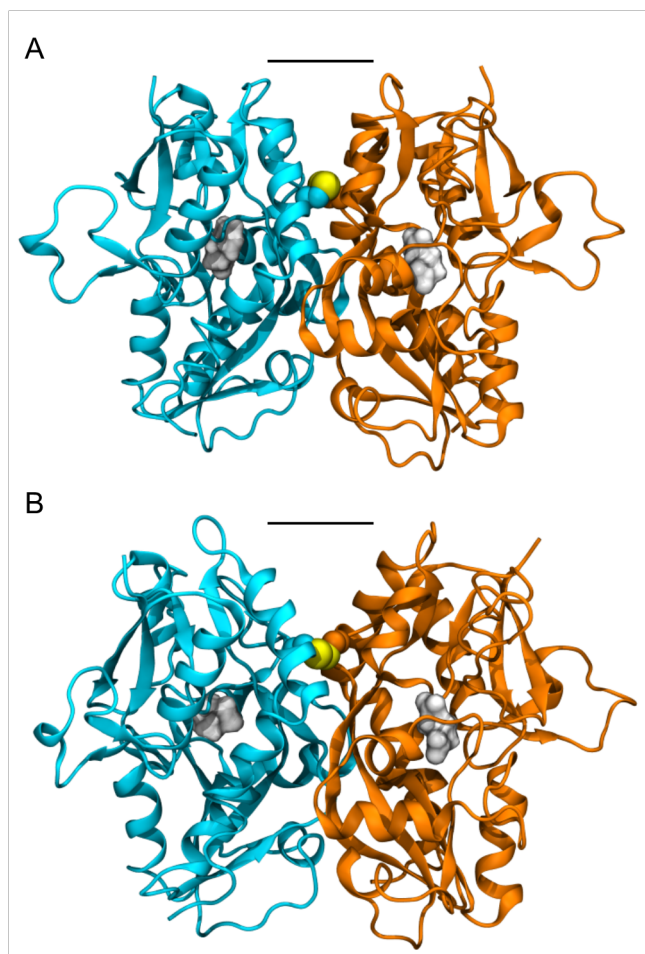


Figure 7. Interface opening of the GluA2 K514C mutant is possible despite the presence of a crosslink. (A) The modelled K514C crosslinked mutant before SMD simulations. C514 is shown in vdW representation. (B) As (A) but after SMD simulation. The black bar highlights the interface opening.

We studied the K514C mutant in both the oxidized and the reduced form. Perhaps surprisingly, we did not observe a large destabilization of the reduced form despite the K514C mutation. The

interface was still fairly stable despite losing the E507-K514 interaction. However, this fits the data of Yelshanskaya *et al.*¹³ showing normal activation of this mutant. Pulling the interface open required work of 74 ± 19 kJ/mol ($n = 4$) which is not significantly different from the GluA2 WT ($p = 0.09$). For the oxidized form, the motion was expected to be limited by the presence of the crosslink. In unbiased simulations, one of the two repeats was very similar to simulations of the WT or K514C in the reduced form with a stable interface. For the other repeat, a rotation of the two chains against one another is observed towards 100 ns (Figure S5). This motion has not been noted for any of the other trajectories. As it disturbs the interface, it could potentially be involved in desensitization, and a rotation motion has indeed been suggested by Yelshanskaya *et al.* as an alternative desensitization mechanism¹³. However, the so-called GT linker distance, which illustrates where the channel-lining helices would be connected to the LBD, increased by 8-10 Å in this rotation motion. This eliminated the possibility that the observed motion is involved in desensitization as the GT linker distance is rather expected to decrease to allow for the channel-lining helices to approach each other for the channel to close. Thus, we believe that this observed conformational change might be an artifact studying the LBD dimer in isolation, as pulling the channel lining helices much further apart than what corresponds to the active state is likely not energetically possible.

The SMD simulations suggested that, despite the restrictions caused by the crosslink, the initial interface opening can still occur to more or less the same degree as observed for GluA2 WT (Figure 7B). The average work for the 2 x 2 SMD repeats was 81 ± 9 kJ/mol ($n = 4$), which was statistically not significantly different from WT ($p = 0.07$). There was some distortion of the protein structure around the K514C residue due to the interface opening, but this is apparently not of high energetic cost.

DISCUSSION AND CONCLUSIONS

By adding external forces to a simulation system, SMD simulations allow the exploration of conformational changes otherwise not obtainable by unbiased MD simulations on the nanosecond timescale. Here we have used SMD to explore the opening of the D1D1 interface for iGluR LBDs, a change likely involved in the desensitization process for these receptors. SMD-type simulations have previously proven useful for exploring protein-protein interfaces, *e.g.* for peptide-peptide interfaces in Alzheimer's amyloid protofibrils and the influence of mutations on the protofibril stability³⁸; for dissociation of a T cell receptor from a major histocompatibility complex presenting a peptide³⁹; and for interface stability of WT and known destabilizing mutants for the Trp-repressor homodimeric protein⁴⁰. The method has also been used for other interfaces, *e.g.* exploring the effect of mutations in the so-called B2 protein on Nodamura virus RNA binding⁴¹.

AMPA receptors and KARs desensitize within milliseconds after being exposed to glutamate. The LBD dimer interface stability critically affects the speed with which the receptors desensitize, and the general understanding is that the interface opens up upon desensitization, allowing the channel-lining helices to close the ion channel (Figure 8). We have shown that for GluK2, where ion binding to the LBD interface is required for activity, unbinding of regulatory ions promoted initial interface opening in unbiased simulations. This interface opening could be pushed further by SMD simulations, and structures obtained by SMD simulations resembled a previously determined crystal structure⁹, which is suggested to be an intermediate between the active and the desensitized states¹². Thus, we suggest that the initial desensitization motions can be studied by SMD simulations. We have furthermore seen that the work required to open the interface in a

given state (ion-bound/ion-free/mutant) correlates with the stability of the active conformation of that given state. If less work is required to push the interface open, the active state of the given receptor is predicted to be less stable (i.e. desensitizes faster) than for a case in which more work is required. From this we suggest, in correspondence with earlier data¹⁹, that the regulatory ions bound in GluK2 have to be released for desensitization to proceed. For AMPARs, where no regulatory ions are required, an important hydrogen bond network across the interface likely needs to be disrupted before desensitization. Furthermore, we see that the GluA2 K514C crosslinked mutant surprisingly seems to be able to undergo at least some interface opening, and at no further energetic cost than the WT GluA2 LBD dimer. Thus, the fact that the crosslinked K514C mutant might desensitize in a way similar to the WT¹³ does not necessarily exclude the possibility of interface opening being involved in desensitization. From the cryo-electron microscopy data presented by Dürr *et al.*¹¹ and Meyerson *et al.*¹² it seems likely that the desensitized state cannot be described by a single conformation, and how much conformational change is required for desensitization to happen is currently unknown. One could imagine a scenario where the initial interface opening would correspond to the initial desensitization, and the structures in which the LBD dimers have disassembled could be more “deeply” desensitized states.

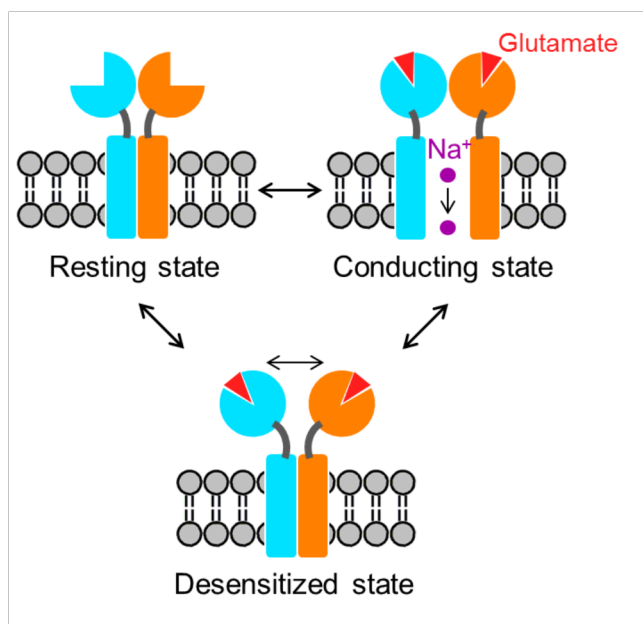


Figure 8. LBD dimer interface opening allows receptor desensitization. Cartoon illustrating a simplified version of the iGluR functional cycle. For clarity, only one dimer is shown, and the ATD is omitted. In the resting state, the LBD dimer interface is probably packed in a way similar to the active state such that ligand binding, inducing clamshell closure, leads to channel opening by pulling the linkers to the transmembrane channel-lining helices. The stability of the active state can be thought of as a competition between the stability of the LBD dimer interface and the strain induced in the TMD from channel opening. Stronger interface interactions can stabilize the active state for longer, while weaker interface interactions allow for faster desensitization, potentially driven by strain in the TMD. Interface opening allows the transmembrane channel to close while glutamate keeps the LBD clamshells in a closed state around the ligand.

For steered MD, and other nonequilibrium work methods, the average of work values for an ensemble of trajectories will be larger than, or equal to, the free energy difference between the

two explored states. The work value obtained for an SMD simulation is path-dependent, and from our data it is seen that the work values reveal the most probable pathway if analyzed in conjunction with the trajectory produced, e.g. that interface-bound ions need to unbind for GluK2 to desensitize and that disruption of the hydrogen bonding network for GluA2 facilitates interface opening.

In principle, one can perform a much larger number of repeats of the SMD simulations and obtain the free energy using Jarzynski's equality⁴². However, it has been argued, based on comparing potentials of mean force obtained by umbrella sampling versus Jarzynski's equality, that Jarzynski's equality is not a practical alternative to more traditional methods to perform free energy calculations in complex biomolecular systems⁴³. For complex systems with many degrees of freedom, the average work values obtained from nonequilibrium work methods such as SMD are likely to be dominated by rare events in which the sampled trajectories correspond to small work values. This means that a large number of repeat simulations, likely more than a hundred³⁹, are required to sample the rare events sufficiently to achieve convergence of the free energy difference^{44,45}.

The non-equilibrium SMD simulations presented here do not investigate all possible pathways between the activated LBD dimer and a state in which the D1D1 interface has opened. Moreover, it cannot be expected to obtain the minimum free-energy pathway from the SMD simulations. However, we do observe clear trends for the work involved in the interface opening following slightly different paths or for different mutants, which matches available experimental data. Therefore, we argue that the simple method of SMD simulations can be used to quantify the stability of the interface to a certain degree of accuracy without having to perform expensive calculations of the free energy change associated with interface opening.

ASSOCIATED CONTENT

Supporting Information

The Supporting Information, Figures S1-S5 and Movie S1, is available free of charge via the Internet at <http://pubs.acs.org>.

Figure S1. RMSD values for GluK2 WT simulations. Figure S2. Ion binding distances for GluK2 WT simulations. Figure S3. Conformational space sampled in eight GluK2 WT SMD simulations and by principal components opening the interface. Figure S4. Interface hydrogen bonding network distances along with work values required to open the GluA2 LBD dimer interface. Figure S5. Rotation at the LBD dimer interface in one unbiased simulations of the crosslinked GluA2 K514C mutant.

Movie S1. Example of a PC showing a component of interface opening.

AUTHOR INFORMATION

Corresponding Authors

* Mailing address: South Parks Road, Oxford, OX1 3QU, United Kingdom. Phone: +44 (0)1865 613304. Email: maria.musgaard@bioch.ox.ac.uk (M.M.)

* Mailing address: South Parks Road, Oxford, OX1 3QU, United Kingdom. Phone: +44 (0)1865 613305. Email: philip.biggin@bioch.ox.ac.uk (P.C.B.)

Notes

The authors declare no competing financial interest.

ACKNOWLEDGMENTS

The work was supported by a grant from the Leverhulme Trust (RPG-059, P.C.B. and M.M.) and M.M. held a postdoctoral fellowship from the Alfred Benzon Foundation. The authors acknowledge the use computer time on ARCHER UK National Supercomputing Service (<http://archer.ac.uk>) granted via the UK High-End Computing Consortium for Biomolecular Simulation, HECBioSim (<http://hecbiosim.ac.uk>), supported by EPSRC (grant no. EP/L000253/1); on HECToR, the UK's National high-performance computing service, which was provided by UoE HPCx Ltd at the University of Edinburgh, Cray Inc and NAG Ltd, and funded by the Office of Science and Technology through EPSRC's High End Computing Programme; on the University of Oxford Advanced Research Computing (ARC) facility (<http://dx.doi.org/10.5281/zenodo.22558>); and on the IRIDIS High Performance Computing Facility at the University of Southampton. Teresa Paramo and Rémi Cuchillo from the Biggin laboratory are thanked for helpful discussions along with Derek Bowie and members of his laboratory at McGill University, Canada.

REFERENCES

- (1) Traynelis, S. F.; Wollmuth, L. P.; McBain, C. J.; Menniti, F. S.; Vance, K. M.; Ogden, K. K.; Hansen, K. B.; Yuan, H.; Myers, S. J.; Dingledine, R. Glutamate Receptor Ion Channels: Structure, Regulation, and Function. *Pharmacol. Rev.* **2010**, 62, 405–496.

- (2) Hollmann, M. Cloned Glutamate Receptors. *Annu. Rev. Neurosci.* **1994**, *17*, 31–108.
- (3) Sobolevsky, A. I.; Rosconi, M. P.; Gouaux, E. X-Ray Structure, Symmetry and Mechanism of an AMPA-Subtype Glutamate Receptor. *Nature* **2009**, *462*, 745–756.
- (4) Lomize, M. A.; Lomize, A. L.; Pogozheva, I. D.; Mosberg, H. I. OPM: Orientations of Proteins in Membranes Database. *Bioinformatics* **2006**, *22*, 623–625.
- (5) Chaudhry, C.; Weston, M. C.; Schuck, P.; Rosenmund, C.; Mayer, M. L. Stability of Ligand-Binding Domain Dimer Assembly Controls Kainate Receptor Desensitization. *EMBO J.* **2009**, *28*, 1518–1530.
- (6) Greger, I. H.; Akamine, P.; Khatri, L.; Ziff, E. B. Developmentally Regulated, Combinatorial RNA Processing Modulates AMPA Receptor Biogenesis. *Neuron* **2006**, *51*, 85–97.
- (7) Sun, Y.; Olson, R.; Horning, M.; Armstrong, N.; Mayer, M.; Gouaux, E. Mechanism of Glutamate Receptor Desensitization. *Nature* **2002**, *417*, 245–253.
- (8) Horning, M. S.; Mayer, M. L. Regulation of AMPA Receptor Gating by Ligand Binding Core Dimers. *Neuron* **2004**, *41*, 379–388.
- (9) Armstrong, N.; Jasti, J.; Beich-Frandsen, M.; Gouaux, E. Measurement of Conformational Changes Accompanying Desensitization in an Ionotropic Glutamate Receptor. *Cell* **2006**, *127*, 85–97.
- (10) Schauder, D. M.; Kuybeda, O.; Zhang, J.; Klymko, K.; Bartesaghi, A.; Borgnia, M. J.; Mayer, M. L.; Subramaniam, S. Glutamate Receptor Desensitization Is Mediated by

- Changes in Quaternary Structure of the Ligand Binding Domain. *Proc. Natl. Acad. Sci. USA* **2013**, *110*, 5921–5926.
- (11) Dürr, K. L.; Chen, L.; Stein, R. A.; De Zorzi, R.; Folea, I. M.; Walz, T.; Mchaourab, H. S.; Gouaux, E. Structure and Dynamics of AMPA Receptor GluA2 in Resting, Pre-Open, and Desensitized States. *Cell* **2014**, *158*, 778–792.
 - (12) Meyerson, J. R.; Kumar, J.; Chittori, S.; Rao, P.; Pierson, J.; Bartesaghi, A.; Mayer, M. L.; Subramaniam, S. Structural Mechanism of Glutamate Receptor Activation and Desensitization. *Nature* **2014**, *514*, 328–334.
 - (13) Yelshanskaya, M. V.; Li, M.; Sobolevsky, A. I. Structure of an Agonist-Bound Ionotropic Glutamate Receptor. *Science* **2014**, *345*, 1070–1074.
 - (14) Lau, A. Y.; Roux, B. The Free Energy Landscapes Governing Conformational Changes in a Glutamate Receptor Ligand-Binding Domain. *Structure* **2007**, *15*, 1203–1214.
 - (15) Lau, A. Y.; Roux, B. The Hidden Energetics of Ligand Binding and Activation in a Glutamate Receptor. *Nat. Struct. Mol. Biol.* **2011**, *18*, 283–287.
 - (16) Yao, Y.; Belcher, J.; Berger, A. J.; Mayer, M. L.; Lau, A. Y. Conformational Analysis of NMDA Receptor GluN1, GluN2, and GluN3 Ligand-Binding Domains Reveals Subtype-Specific Characteristics. *Structure* **2013**, *21*, 1788–1799.
 - (17) Plested, A. J. R.; Vijayan, R.; Biggin, P. C.; Mayer, M. L. Molecular Basis of Kainate Receptor Modulation by Sodium. *Neuron* **2008**, *58*, 720–735.
 - (18) Vijayan, R.; Plested, A. J. R.; Mayer, M. L.; Biggin, P. C. Selectivity and Cooperativity of

- Modulatory Ions in a Neurotransmitter Receptor. *Biophys. J.* **2009**, *96*, 1751–1760.
- (19) Dawe, G. B.; Musgaard, M.; Andrews, E. D.; Daniels, B. A.; Aurousseau, M. R. P.; Biggin, P. C.; Bowie, D. Defining the Structural Relationship between Kainate-Receptor Deactivation and Desensitization. *Nat. Struct. Mol. Biol.* **2013**, *20*, 1054–1061.
- (20) Dawe, G. B.; Musgaard, M.; Aurousseau, M. R. P.; Nayeem, N.; Green, T.; Biggin, P. C.; Bowie, D. Distinct Structural Pathways Coordinate the Activation of AMPA Receptor-Auxiliary Subunit Complexes. *Neuron* **2016**, *89*, 1264–1276.
- (21) Wong, A. Y. C.; Fay, A.-M. L.; Bowie, D. External Ions Are Coactivators of Kainate Receptors. *J. Neurosci.* **2006**, *26*, 5750–5755.
- (22) Weston, M. C.; Schuck, P.; Ghosal, A.; Rosenmund, C.; Mayer, M. L. Conformational Restriction Blocks Glutamate Receptor Desensitization. *Nat. Struct. Mol. Biol.* **2006**, *13*, 1120–1127.
- (23) Nayeem, N.; Mayans, O.; Green, T. Conformational Flexibility of the Ligand-Binding Domain Dimer in Kainate Receptor Gating and Desensitization. *J. Neurosci.* **2011**, *31*, 2916–2924.
- (24) Sali, A.; Blundell, T. L. Comparative Protein Modelling by Satisfaction of Spatial Restraints. *J. Mol. Biol.* **1993**, *234*, 779–815.
- (25) Jorgensen, W. L.; Maxwell, D. S.; Tirado-Rives, J. Development and Testing of the OLPS All-Atom Force Field on Conformational Energetics and Properties of Organic Liquids. *J. Am. Chem. Soc.* **1996**, *118*, 11225–11236.

- (26) Kaminski, G. a; Friesner, R. a; Tirado-rives, J.; Jorgensen, W. L. Comparison with Accurate Quantum Chemical Calculations on Peptides †. *J. Phys. Chem. B* **2001**, *105*, 6474–6487.
- (27) Jorgensen, W. L.; Chandrasekhar, J.; Madura, J. D.; Impey, R. W.; Klein, M. L. Comparison of Simple Potential Functions for Simulating Liquid Water. *J. Chem. Phys.* **1983**, *79*, 926-935.
- (28) Hess, B.; Kutzner, C.; van der Spoel, D.; Lindahl, E. GROMACS 4: Algorithms for Highly Efficient, Load-Balanced, and Scalable Molecular Simulation. *J. Chem. Theory Comput.* **2008**, *4*, 435–447.
- (29) Berendsen, H. J. C.; Postma, J. P. M.; van Gunsteren, W. F.; DiNola, A.; Haak, J. R. Molecular Dynamics with Coupling to an External Bath. *J. Chem. Phys.* **1984**, *81*, 3684–3690.
- (30) Darden, T.; York, D.; Pedersen, L. Particle Mesh Ewald: An N·log(N) Method for Ewald Sums in Large Systems. *J. Chem. Phys.* **1993**, *98*, 10089-10092.
- (31) Essmann, U.; Perera, L.; Berkowitz, M. L.; Darden, T.; Lee, H.; Pedersen, L. G. A Smooth Particle Mesh Ewald Method. *J Chem Phys* **1995**, *103*, 8577–8593.
- (32) Hess, B. P-LINCS: A Parallel Linear Constraint Solver for Molecular Simulation. *J. Chem. Theory Comput.* **2008**, *4*, 116–122.
- (33) Bonomi, M.; Branduardi, D.; Bussi, G.; Camilloni, C.; Provasi, D.; Raiteri, P.; Donadio, D.; Marinelli, F.; Pietrucci, F.; Broglia, R. A.; Parrinello, M. PLUMED: A Portable Plugin for Free-Energy Calculations with Molecular Dynamics. *Comput. Phys. Commun.* **2009**,

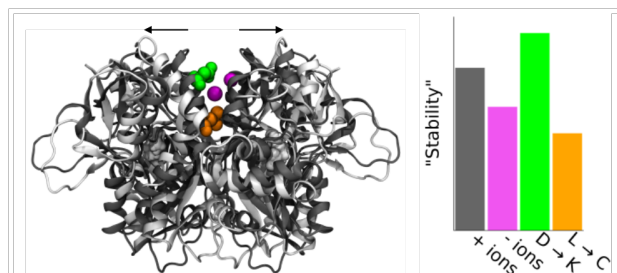
180, 1961–1972.

- (34) Humphrey, W.; Dalke, A.; Schulten, K. VMD: Visual Molecular Dynamics. *J. Mol. Graph.* **1996**, *14*, 33–38.
- (35) Plested, A. J. R.; Mayer, M. L. Structure and Mechanism of Kainate Receptor Modulation by Anions. *Neuron* **2007**, *53*, 829–841.
- (36) Nayeem, N.; Zhang, Y.; Schweppe, D. K.; Madden, D. R.; Green, T. A Nondesensitizing Kainate Receptor Point Mutant. *Mol. Pharmacol.* **2009**, *76*, 534–542.
- (37) Bowie, D. External Anions and Cations Distinguish between AMPA and Kainate Receptor Gating Mechanisms. *J. Physiol.* **2002**, *539.3*, 725–733.
- (38) Lemkul, J. A.; Bevan, D. R. Assessing the Stability of Alzheimer’s Amyloid Protofibrils Using Molecular Dynamics. *J. Phys. Chem. B* **2010**, *114*, 1652–1660.
- (39) Cuendet, M. A.; Michielin, O. Protein-Protein Interaction Investigated by Steered Molecular Dynamics: The TCR-pMHC Complex. *Biophys. J.* **2008**, *95*, 3575–3590.
- (40) Miño, G.; Baez, M.; Gutierrez, G. Effect of Mutation at the Interface of Trp-Repressor Dimeric Protein: A Steered Molecular Dynamics Simulation. *Eur. Biophys. J.* **2013**, *42*, 683–690.
- (41) Allen, W. J.; Wiley, M. R.; Myles, K. M.; Adelman, Z. N.; Bevan, D. R. Steered Molecular Dynamics Identifies Critical Residues of the Nodamura Virus B2 Suppressor of RNAi. *J. Mol. Model.* **2014**, *20*, 2092.
- (42) Jarzynski, C. Nonequilibrium Equality for Free Energy Differences. *Phys. Rev. Lett.* **1997**,

78, 2690–2693.

- (43) Baştuğ, T.; Kuyucak, S. Application of Jarzynski's Equality in Simple versus Complex Systems. *Chem. Phys. Lett.* **2007**, *436*, 383–387.
- (44) Pohorille, A.; Jarzynski, C.; Chipot, C. Good Practices in Free-Energy Calculations. *J. Phys. Chem. B* **2010**, *114*, 10235–10253.
- (45) Park, S.; Khalili-Araghi, F.; Tajkhorshid, E.; Schulten, K. Free Energy Calculation from Steered Molecular Dynamics Simulations Using Jarzynski's Equality. *J. Chem. Phys.* **2003**, *119*, 3559–3566.

For “Table of Contents” use only.



Steered Molecular Dynamics Simulations Predict Conformational Stability of Glutamate Receptors

Maria Musgaard and Philip C. Biggin**

Department of Biochemistry, University of Oxford, Oxford, United Kingdom